Pergamon

Int. J. Solids Structures Vol. 33, No. 3, pp. 343–359, 1996

0020-7683/96 $9.50 + .00

0020-7683(95)00046-1

FRACTURE MECHANICS FOR A MODE III CRACK IN A PIEZOELECTRIC MATERIAL

TONG-YI ZHANG and PIN TONG
Department of Mechanical Engineering, Centre for Advanced Engineering Materials, Hong Kong University of Science and Technology, Clear Water Bay, Kowloon, Hong Kong

(*Received* 20 *July* 1994; *in revised form* 14 *February* 1995)

Abstract—The mechanical and electric fields in a piezoelectric material around an elliptical cylinder cavity and the electric field within the cavity are formulated by complex potentials. The electric field inside the cavity is uniform and varies with the shape of the ellipse. When the cavity is reduced to a slit crack, the electric field strength inside the cavity is inversely proportional to the permittivity of the cavity. When the ratio of the short semi-axis of the ellipse over the long semi-axis is much smaller than the ratio of the permittivity of the cavity over that of the material, it can be used as the electric boundary condition that the electric field strength along the crack faces equals the remote one. In this case, the energy release rate for crack propagation depends only on the applied stress and can be represented in terms of the stress intensity factor as in a pure elastic body without coupling with the electric field. Electric loading may promote or retard crack propagation depending on whether it increases or decreases the applied stress.

1. INTRODUCTION

In 1976, Parton published a fundamental result on the fracture mechanics of piezoelectric materials. He assumed that a crack was a traction-free but permeable slit, with the electric potential and the normal component of the electric displacement continuous across the slit. Since the permittivity of a piezoelectric material may be three orders of magnitude higher than that of air or vacuum, the electric potential at the upper crack face may be different from that at the lower face. Therefore, the boundary conditions used there may not appear to have strong physical support. In 1980, Deeg analysed dislocation, crack and inclusion problems in piezoelectric solids. To simplify the mathematical evaluation, Deeg proposed that the normal component of the electric displacement could be treated as zero at the upper and lower crack faces. In order to prove the validity of Deeg's approximation, Pak (1990) gave a detailed argument for neglecting the electric displacement within the crack. This boundary condition may be called the D-P condition. Currently, the D-P condition predominates in studying the fracture mechanics of piezoelectric materials. Using the D-P condition, Pak (1990) studied a crack with its front coincident with the poling axis. Sosa and Pak (1990) investigated a more general crack tip field using an eigenfunction analysis. Shindo *et al.* (1990) analysed cracks in piezoelectric layers using integral equation methods. Kuo and Barnett (1991) carried out an asymptotic crack tip analysis. Pak (1992) and Suo *et al.* (1992) reanalysed the stress and electric fields near a finite crack. The D-P boundary condition leads to singularities of the electric displacement and the electric field strength at crack tips. Two assumptions are involved in the D-P boundary condition, namely: (1) no free charge resides on either crack face; and (2) the electric displacement within the crack is negligible.

In 1989 McMeeking calculated electrostrictive stresses near a crack tip. His results show that if the aspect ratio of a flaw thickness to length is an order of magnitude larger than the dielectric permittivity of the interior of the flaw divided by the dielectric permittivity of the surrounding material, then a model using an electrically impermeable flaw is appropriate. As the flaw ratio diminishes, the effective mechanical stress intensity factor approaches zero (McMeeking, 1989). Pak and Tobin (1993) studied crack face boundary conditions for piezoelectric materials. They found that the ratio of the crack tip electric

field to the applied field approaches unity as an elliptical cavity reduces to a slit crack, and the crack tip electric field had multiple values for different limiting processes.

The electric boundary conditions along an interface should be the continuity of the normal component of the electric displacement and the continuity of the tangent component of the electric field strength (Jackson, 1976). Using such boundary conditions, Zhang and Hack (1992) have analysed the fracture of a mode III crack. However, the electric field within a slit crack could not be studied by Zhang and Hack (1992), because the volume of the slit crack is treated as zero. Recently, Zhang (1994a) investigated the effect of sample width on the energy release rate for crack propagation. The results show that the energy release rate varies with the aspect ratio of the sample width to the crack width, because both electric field strength and electric energy change with the crack width.

To establish a fundamentally sound solution for a slit-like crack, we consider an elliptical hole in the present work. When the short semi-axis of the ellipse approaches zero, we obtain the solution for a sharp crack. From the limiting process we can study the effects of different sized gaps between the crack faces and varying permittivity within the crack. When the crack front coincides with the poling axis, the in-plane deformation is decoupled from the anti-plane deformation and the in-plane electric field. Therefore, we study an elliptical cavity under anti-plane mechanical loading and in-plane electric loading in the present work, because the anti-plane deformation is always coupled with the electric field.

Barnett and Lothe (1975), Suo *et al.* (1992), Sosa and Pak (1990), Pak (1992) and Park (1994) formulated the general solution to the mechanical and electric coupling problems. Sosa (1993) reviewed the crack problems in piezoelectric ceramics. Dunn (1994) investigated the effects of crack face boundary conditions on the fracture mechanics of piezoelectric solids. More recently, Zhang (1994b) proposed a test to measure the isothermal J-integral by using multiple samples with identical geometry but different crack length. His results indicate that the isothermal virtual work equals the virtual change of the full Gibbs function (Zhang, 1994b). The J-integral for piezoelectric materials can be derived from the displacement–force and charge–voltage curves which are recorded during testing (Zhang, 1994b). Using the full Gibbs function, Zhang and Tong (1995) solved the fracture problems in piezoelectric materials. The results show that the energy release rate is positively definite, which is consistent with the present work. The present study emphasizes mode III cracks and our new work (Zhang and Tong, 1995) will report results for general cases.

2. ANTI-PLANE STRAIN EQUATIONS

The three-dimensional formulation of linear piezoelectricity is briefly summarized here. Following Parton and Kudryavtsev (1988), the governing field equations at constant temperature are given by:

$$\begin{aligned} \boldsymbol{\sigma}_{ij,j} &= \mathbf{0}, \\ \mathbf{D}_{i,i} &= \mathbf{0}. \end{aligned} \tag{1}$$

with boundary conditions along an interface between a gas (or vacuum) phase and a piezoelectric solid:

$$\begin{aligned} \boldsymbol{\sigma} \cdot \mathbf{n} &= \mathbf{T}, \\ (\mathbf{D}^{\mathrm{m}} - \mathbf{D}^{\mathrm{c}}) \cdot \mathbf{n} &= -q, \\ (\mathbf{E}^{\mathrm{m}} - \mathbf{E}^{\mathrm{c}}) \times \mathbf{n} &= 0, \end{aligned} \tag{2}$$

and constitutive equations:

$$\begin{aligned} \boldsymbol{\sigma}_{ij} &= c_{ijkl}\mathbf{s}_{kl} - e_{kij}\mathbf{E}_k, \\ \mathbf{D}_i &= e_{ikl}\mathbf{s}_{kl} + \varepsilon_{ik}\mathbf{E}_k, \end{aligned} \tag{3}$$

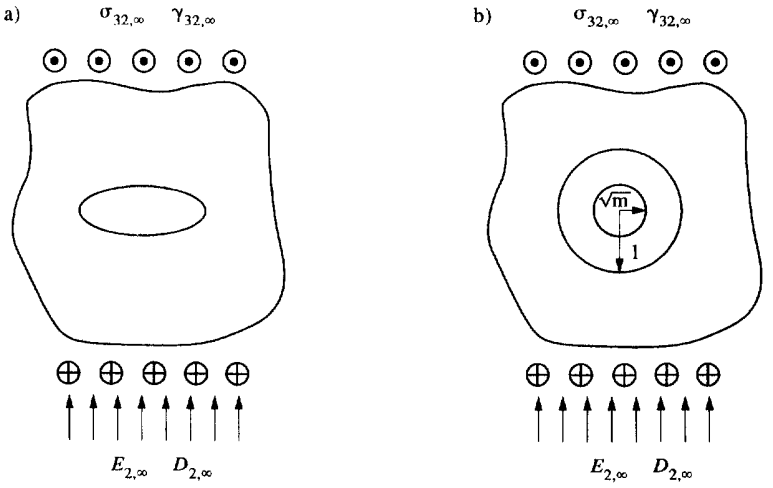

Fig. 1. (a) Remote mechanical and electric loads in the z plane. (b) Mapping the elliptical cavity into a unit circle in the ζ plane.

where the superscripts m and c refer to "in material" and "in air or vacuum", respectively, $\boldsymbol{\sigma}_{ij}$ and $\mathbf{s}_{ij}$ are the stress and strain tensors, respectively, c_{ijkl} are the elastic moduli measured at a constant electric field, ε_{ij} are the dielectric constants measured at constant strain, e_{ikl} are the piezoelectric constants, $\mathbf{E}_k$ and $\mathbf{D}_k$ are the electric field strength and the electric displacement vectors, respectively, q is the density of free charge on the surface between the two media, $\mathbf{T}$ is traction along the boundary and $\mathbf{n}$ is the unit vector normal to the boundary.

The piezoelectric effect is found only in crystals which do not possess a centre of symmetry. For the purposes of illustration and comparison with previous works (Pak, 1990; Zhang and Hack, 1992), we will consider a transversely isotropic material belonging to the hexagonal crystal class *6mm*. In contracted notation, the governing equations for the anti-plane strain problem (only out-of-plane displacements and in-plane electric fields) in such a material containing an elliptical hole ($x_1^2/a^2 + x_2^2/b^2 = 1$), as shown in Fig. 1(a), reduce to:

$$\begin{aligned} c_{44}\nabla^2 u_3 + e_{15}\nabla^2\phi &= 0, \\ e_{15}\nabla^2 u_3 - \varepsilon_{11}\nabla^2\phi &= 0, \end{aligned} \tag{4}$$

where ∇^2 is the two-dimensional Laplacian operator, u_3 is the displacement in the x_3 direction and ϕ is the static electrical potential. We define:

$$\begin{aligned} \gamma_{31} &= \frac{\partial u_3}{\partial x_1}, \quad \gamma_{32} = \frac{\partial u_3}{\partial x_2}, \\ \mathbf{E}_1 &= -\frac{\partial \phi}{\partial x_1}, \quad \mathbf{E}_2 = -\frac{\partial \phi}{\partial x_2}, \end{aligned} \tag{5}$$

where $\gamma_{31} = 2\mathbf{s}_{31}$ and $\gamma_{32} = 2\mathbf{s}_{32}$. Let u_3 and ϕ be the imaginary parts of the analytic complex functions U and Φ, such that:

$$\begin{aligned} u_3 &= \mathscr{I}[U(z)], \\ \phi &= \mathscr{I}[\Phi(z)], \end{aligned} \tag{6}$$

where $z = x_1 + \mathrm{i}x_2$. Then, the governing equations are automatically satisfied. Defining the

complex strain, γ, the complex electric field strength, $\mathbf{E}$, the complex stress, $\boldsymbol{\sigma}$, and the complex electric displacement, $\mathbf{D}$, as:

$$\gamma = \gamma_{32} + i\gamma_{31}, \quad \mathbf{E} = \mathbf{E}_2 + i\mathbf{E}_1,$$
$$\boldsymbol{\sigma} = \boldsymbol{\sigma}_{32} + i\boldsymbol{\sigma}_{31}, \quad \mathbf{D} = \mathbf{D}_2 + i\mathbf{D}_1, \tag{7}$$

we can represent the constitutive equations as:

$$\boldsymbol{\sigma} = c_{44} U'(z) + e_{15} \Phi'(z),$$
$$\mathbf{D} = e_{15} U'(z) - \varepsilon_{11} \Phi'(z), \tag{8}$$

where prime denotes differentiation with respect to z.

The boundary conditions along the surface of the elliptical hole have the form:

$$\boldsymbol{\sigma}_\perp = \mathbf{0} \quad \text{(traction-free)},$$
$$\mathbf{D}_\perp^m = \mathbf{D}_\perp^c \quad \text{(surface charge-free)},$$
$$\mathbf{E}_\parallel^m = \mathbf{E}_\parallel^c \quad \text{(irrotationality of electric fields)}, \tag{9}$$

where the subscripts $\perp$ and $\parallel$ mean, respectively, perpendicular and parallel to the surface.

Consider the conformal mapping function

$$z = R\left(\zeta + \frac{m}{\zeta}\right)$$

where

$$R = \frac{a+b}{2} \text{ and } m = \frac{a-b}{a+b}, \tag{10}$$

which maps the ellipse in the z plane into a unit circle in the ζ plane, and the line segment $(-c, c)$ in the z plane into a circle with a radius of $\sqrt{m}$ in the ζ plane, as shown in Fig. 1(b), where $c^2 = a^2 - b^2$. The inverse mapping function of eqn (10) is

$$\zeta = \frac{z + \sqrt{(z^2 - c^2)}}{2R}. \tag{11}$$

The problem in the z plane can be solved by mapping the elliptical hole into the circular ring in the ζ plane. To ensure that the electric field is single valued along the line segment, the complex potential Φ^e must satisfy the following condition

$$\Phi^e[(\sqrt{m})\, e^{i\theta}] = \Phi^e[(\sqrt{m})\, e^{-i\theta}], \tag{12}$$

where θ is the polar angle.

The three complex potentials in the ζ plane can be expressed in the forms

$$U(\zeta) = A_1 \zeta + \frac{A_2}{\zeta},$$
$$\Phi^m(\zeta) = B_1 \zeta + \frac{B_2}{\zeta},$$
$$\Phi^e(\zeta) = C_1 \zeta + \frac{C_2}{\zeta}. \tag{13}$$

In general, A_1, A_2, B_1, B_2, C_1 and C_2 are complex constants. Since remote electric and mechanical fields are applied only along the x_2 direction in the present study, the six constants can be treated as real. Consequently, the boundary conditions of eqn (9) may be represented in terms of the complex potentials

$$\begin{aligned}
&\mathscr{I}[(c_{44}U'+e_{15}(\Phi^{\mathrm{m}})')\,\mathrm{e}^{\mathrm{i}\theta}] = 0 \quad \text{(traction-free)},\\
&\mathscr{I}[(e_{15}U'-\varepsilon_{11}^{\mathrm{m}}(\Phi^{\mathrm{m}})')\,\mathrm{e}^{\mathrm{i}\theta}] = \mathscr{I}[-\varepsilon_{11}^{\mathrm{c}}(\Phi^{\mathrm{c}})'\,\mathrm{e}^{\mathrm{i}\theta}] \quad \text{(surface charge-free)},\\
&\mathscr{R}[(\Phi^{\mathrm{m}})'\,\mathrm{e}^{\mathrm{i}\theta}] = \mathscr{R}[(\Phi^{\mathrm{c}})'\,\mathrm{e}^{\mathrm{i}\theta}] \quad \text{(irrotationality of electric fields)}. \qquad (14)
\end{aligned}$$

From eqns (12) and (14), we find four relations among these constants.

$$\begin{aligned}
&B_1-B_2 = C_1(1-m), \quad c_{44}(A_1+A_2)+e_{15}(B_1+B_2) = 0,\\
&e_{15}(A_1+A_2)-\varepsilon_{11}^{\mathrm{m}}(B_1+B_2)+\varepsilon_{11}^{\mathrm{c}}C_1(1+m) = 0, \quad C_1 m = C_2. \qquad (15)
\end{aligned}$$

As a result, the constants A_2, B_2, C_1 and C_2 can be expressed in terms of A_1 and B_1

$$\begin{aligned}
A_2 &= \frac{-2(1+m)\varepsilon_{11}^{\mathrm{c}}e_{15}}{(1-m)(e_{15}^2+c_{44}\varepsilon_{11}^{\mathrm{m}})+(1+m)c_{44}\varepsilon_{11}^{\mathrm{c}}}B_1 - A_1 = \frac{-2\beta e_{15}}{(\alpha+\beta)c_{44}}B_1 - A_1,\\
B_2 &= \frac{(1+m)c_{44}\varepsilon_{11}^{\mathrm{c}}-(1-m)(e_{15}^2+c_{44}\varepsilon_{11}^{\mathrm{m}})}{(1-m)(e_{15}^2+c_{44}\varepsilon_{11}^{\mathrm{m}})+(1+m)c_{44}\varepsilon_{11}^{\mathrm{c}}}B_1 = -\frac{\alpha-\beta}{\alpha+\beta}B_1,\\
C_1 &= \frac{2(e_{15}^2+c_{44}\varepsilon_{11}^{\mathrm{m}})}{(1-m)(e_{15}^2+c_{44}\varepsilon_{11}^{\mathrm{m}})+(1+m)c_{44}\varepsilon_{11}^{\mathrm{c}}}B_1 = \frac{1+\alpha}{\alpha+\beta}B_1,\\
C_2 &= \frac{2m(e_{15}^2+c_{44}\varepsilon_{11}^{\mathrm{m}})}{(1-m)(e_{15}^2+c_{44}\varepsilon_{11}^{\mathrm{m}})+(1+m)c_{44}\varepsilon_{11}^{\mathrm{c}}}B_1 = \frac{1-\alpha}{\alpha+\beta}B_1, \qquad (16)
\end{aligned}$$

where α and β are dimensionless constants given by

$$\alpha = \frac{b}{a}, \quad \beta = \frac{\varepsilon_{11}^{\mathrm{c}}}{\varepsilon_{\mathrm{e}}},$$

and

$$\varepsilon_{\mathrm{e}} = \varepsilon_{11}^{\mathrm{m}} + \frac{e_{15}^2}{c_{44}} \qquad (17)$$

is an effective dielectric constant of the material, which was first introduced by Zhang and Hack (1992). The constants A_1 and B_1 can be further determined by the remote loading conditions. As studied in previous works (Pak, 1990; Zhang and Hack, 1992), there are four cases of combined electric and mechanical loadings. These are:

(1) a remote mechanical stress component, $\sigma_{32,\infty}$, and a remote electric displacement, $D_{2,\infty}$, along the x_2 axis;

(2) a remote mechanical strain component, $\gamma_{32,\infty}$, and a remote electric field strength, $E_{2,\infty}$, along the x_2 axis;

(3) a remote mechanical stress component, $\sigma_{32,\infty}$, and a remote electric field strength, $E_{2,\infty}$, along the x_2 axis; and

(4) a remote mechanical strain component, $\gamma_{32,\infty}$, and a remote electric displacement, $D_{2,\infty}$, along the x_2 axis.

The four loading cases are illustrated in Figs 1(a, b). For case 1, eqn (8) may be expressed as

$$\lim_{z \to \gamma} \sigma = c_{44} U' + e_{15} (\Phi^{\mathrm{m}})' = \sigma_{32,\infty},$$

$$\lim_{z \to \gamma} D = e_{15} U' - \varepsilon_{11}^{\mathrm{m}} (\Phi^{\mathrm{m}})' = D_{2,\infty}. \tag{18}$$

Substituting eqn (13) into eqn (18), we have

$$c_{44} A_1 + e_{15} B_1 = \sigma_{32,\infty}, \quad e_{15} A_1 - \varepsilon_{11}^{\mathrm{m}} B_1 = D_{2,\infty}. \tag{19}$$

Solving eqn (19) results in the two constants A_1 and B_1

$$A_1 = \frac{\varepsilon_{11}^{\mathrm{m}} \sigma_{32,\infty} + e_{15} D_{2,\infty}}{e_{15}^2 + c_{44} \varepsilon_{11}^{\mathrm{m}}} = \frac{\sigma_{32,\infty}}{\mu_{\mathrm{e}}} + \frac{D_{2,\infty}}{e_{\mathrm{e}}},$$

$$B_1 = \frac{e_{15} \sigma_{32,\infty} - c_{44} D_{2,\infty}}{e_{15}^2 + c_{44} \varepsilon_{11}^{\mathrm{m}}} = \frac{\sigma_{32,\infty}}{e_{\mathrm{e}}} - \frac{D_{32,\infty}}{\varepsilon_{\mathrm{e}}}, \tag{20}$$

where μ_{e} and e_{e} are the effective shear modulus and effective piezoelectric constant, respectively, which are given by

$$\mu_{\mathrm{e}} = c_{44} + e_{15}^2 / \varepsilon_{11}^{\mathrm{m}}, \quad e_{\mathrm{e}} = c_{44} \varepsilon_{\mathrm{e}} / e_{15} = \mu_{\mathrm{e}} \varepsilon_{11}^{\mathrm{m}} / e_{15} = e_{15} + c_{44} \varepsilon_{11}^{\mathrm{m}} / e_{15}. \tag{21}$$

Analogous to case 1, the two constants A_1 and B_1 for the remaining three cases are determined and expressed as:

$$A_1 = \gamma_{32,\infty}, \quad B_1 = -E_{2,\infty} \quad \text{for case 2,}$$

$$A_1 = \frac{\sigma_{32,\infty} + e_{15} E_{2,\infty}}{c_{44}} = \gamma_{32,\infty}, \quad B_1 = -E_{2,\infty} \text{ for case 3,}$$

$$A_1 = \gamma_{32,\infty}, \quad B_1 = \frac{e_{15} \gamma_{32,\infty} - D_{2,\infty}}{\varepsilon_{11}^{\mathrm{m}}} = -E_{2,\infty} \quad \text{for case 4.} \tag{22}$$

For each of the four loading cases, A_1 and B_1 denote the remote strain and electric fields, respectively.

The complex potentials in the z plane result from the corresponding ones in the ζ plane by multiplying by R. They are given by

$$U(z) = R\left[A_1 \zeta(z) + \frac{A_2}{\zeta(z)} \right],$$

$$\Phi^{\mathrm{m}}(z) = R\left[B_1 \zeta(z) + \frac{B_2}{\zeta(z)} \right],$$

$$\Phi^{\mathrm{c}}(z) = R\left[C_1 \zeta(z) + \frac{C_2}{\zeta(z)} \right]. \tag{23}$$

From the inverse conformal mapping function, eqn (11), we have

$$\frac{\mathrm{d}\zeta}{\mathrm{d}z} = \frac{1}{2R} \frac{z + \sqrt{(z^2 - c^2)}}{\sqrt{(z^2 - c^2)}}. \tag{24}$$

Differentiating the three complex potentials leads to the strain and electric fields

$$\gamma = U'(z) = \left[\frac{A_1[z+\sqrt{(z^2-c^2)}]}{2} - \frac{2R^2A_2}{z+\sqrt{(z^2-c^2)}}\right]\frac{1}{\sqrt{(z^2-c^2)}},$$

$$-\mathbf{E}^{\mathrm{m}} = (\Phi^{\mathrm{m}})'(z) = \left[\frac{B_1[z+\sqrt{(z^2-c^2)}]}{2} - \frac{2R^2B_2}{z+\sqrt{(z^2-c^2)}}\right]\frac{1}{\sqrt{(z^2-c^2)}},$$

$$-\mathbf{E}^{\mathrm{c}} = (\Phi^{\mathrm{c}})'(z) = C_1. \quad (25)$$

It can be seen in eqn (25) that the electric field inside the hole is uniform and varies with m. Now it is straightforward to derive the stress field and the electric displacements by using the constitutive equations, i.e. eqns (8).

3. ELECTRIC FIELD INSIDE THE ELLIPTICAL CAVITY

The electric field strength within the elliptical hole equals the constant C_1 but with an opposite sign, which can be rewritten as

$$\mathbf{E}^{\mathrm{c}} = \frac{1+\alpha}{\alpha+\beta}E_{2,\infty}. \quad (26)$$

Equation (26) shows that the electric field strength inside the cavity is uniform and has a finite value. Suppose that the permittivity inside the hole is much smaller than that of the material. In this case, β approaches zero, then eqn (26) reduces to

$$\mathbf{E}^{\mathrm{c}} = \frac{1+\alpha}{\alpha}E_{2,\infty}. \quad (27)$$

In this limit, the electric field strength inside the hole is very sensitive to α. The electric field strength approaches infinity when $\alpha \to 0$. If $\alpha \to 0$ first, eqn (26) approximates to

$$\mathbf{E}^{\mathrm{c}} = \frac{\varepsilon_{\mathrm{e}}}{\varepsilon_{11}^{\mathrm{c}}}E_{2,\infty}. \quad (28)$$

It is indicated in eqn (28) that the electric field strength inside the hole is inversely proportional to the permittivity of the hole in this case. If the permittivity of the hole approaches zero, then the electric field strength will become infinite.

The electric displacement within the hole is the product of the electric field strength times the permittivity of the hole. From eqn (26), we have

$$\mathbf{D}^{\mathrm{c}} = \frac{1+\alpha}{1+\alpha/\beta}\varepsilon_{\mathrm{e}}E_{2,\infty}. \quad (29)$$

As can be seen in eqn (29), the electric displacement inside the cavity is also uniform. There are three limits when α approaches zero. They are:

$$\mathbf{D}^{\mathrm{c}} = \varepsilon_{\mathrm{e}}E_{2,\infty} \quad \text{for } \alpha \to 0 \text{ and } \alpha/\beta \to 0,$$

$$\mathbf{D}^{\mathrm{c}} = \frac{\varepsilon_{\mathrm{e}}E_{2,\infty}}{\alpha/\beta+1} \quad \text{for } \alpha \to 0 \text{ and } \alpha/\beta \to \text{constant},$$

$$\mathbf{D}^{\mathrm{c}} \to 0 \quad \text{for } \alpha \to 0 \text{ and } \alpha/\beta \to \infty. \quad (30)$$

Equation (30) indicates that the electric displacement may approach zero only when the ratio of α/β approaches infinity. For the other two limits the electric displacement is larger than zero.

As described above, both the electric field strength and the electric displacement inside the cavity are uniform and have only one component parallel to the x_2 axis. When the cavity reduces to a slit crack, its volume approaches zero. The electric energy density inside the hole may approach infinity if the electric field strength approaches infinity. In this case, the electric energy of the cavity is not trivial, which will have a great influence on the energy release rate for crack propagation.

4. ELECTRIC FIELD ALONG THE ELLIPTICAL CAVITY SURFACE

The electric field strength within a piezoelectric material is given in eqn (24). Substituting B_2 into eqn (25), we have

$$\mathbf{E}^{\mathrm{m}} = \frac{E_{2,\infty}}{2\sqrt{(z^2-c^2)}}\left[z+\sqrt{(z^2-c^2)}+\frac{(a+b)(\alpha-\beta)}{(\alpha+\beta)[z+\sqrt{(z^2-c^2)}]}\right]. \tag{31}$$

Along the elliptical surface, $z = a\cos\theta + \mathrm{i}b\sin\theta$, and then the electric field strength may be expressed in terms of the parameter θ

$$\mathbf{E}^{\mathrm{m}} = \frac{E_{2,\infty}(1+\alpha)}{2(\alpha\cos\theta+\mathrm{i}\sin\theta)}\left[\mathrm{e}^{\mathrm{i}\theta}+\frac{(\alpha-\beta)\,\mathrm{e}^{-\mathrm{i}\theta}}{\alpha+\beta}\right]. \tag{32}$$

As expected, $\mathbf{E}^{\mathrm{m}} = \mathbf{E}^{\mathrm{c}}$ for $\theta = 0$ and $\theta = \pi$. When α approaches zero, eqn (32) is reduced to

$$\mathbf{E}^{\mathrm{m}} = E_{32,\infty}. \tag{33}$$

Equation (33) shows that the electric field strength is uniform along the crack surfaces and equals the remote applied electric field strength. This phenomenon was found before by Pak and Tobin (1993). This result may be used as a boundary condition to solve fracture problems for long slit cracks.

When β approaches zero first, then eqn (32) is reduced to

$$\mathbf{E}^{\mathrm{m}} = \frac{E_{2,\infty}(1+\alpha)\cos\theta}{\alpha\cos\theta+\mathrm{i}\sin\theta}. \tag{34}$$

Then, letting α approach zero reduces eqn (34) further to

$$\mathbf{E}^{\mathrm{m}} = -\mathrm{i}E_{2,\infty}\cot\theta. \tag{35}$$

As can be seen in eqns (33) and (35), the two approachings result in two different solutions. Equation (35) shows that the electric field strength has a singularity when $\theta = 0$ and the electric field strength only has a component along the x_1 direction, which contrasts to that directly derived from eqn (32). If β is treated as zero first and then α approaches zero, the electric field strengths along the elliptical surface have, respectively, an infinite value of component E_2 when the surfaces are approached from the inside of the hole, as shown in eqn (26), and variable values of component E_1 when the surfaces are approached from the outside, as shown in eqn (35).

The electric displacement in the material is calculated by using eqns (8) and (25). It turns out as

$$\mathbf{D}^{\mathrm{m}} = \left[\frac{A_1[z+\sqrt{(z^2-c^2)}]}{2} - \frac{2R^2A_2}{z+\sqrt{(z^2-c^2)}}\right]\frac{e_{15}}{\sqrt{(z^2-c^2)}} - \left[\frac{B_1[z+\sqrt{(z^2-c^2)}]}{2} - \frac{2R^2B_2}{z+\sqrt{(z^2-c^2)}}\right]\frac{\varepsilon_{11}^{\mathrm{m}}}{\sqrt{(z^2-c^2)}}. \quad (36)$$

Along the hole surface, the electric displacement has the following form:

$$\mathbf{D}^{\mathrm{m}} = \frac{1+\alpha}{\alpha\cos\theta+\mathrm{i}\sin\theta}\left[e_{15}\gamma_{32,z}\cos\theta - \frac{e_{15}\beta\mathrm{e}^{\mathrm{i}\theta}}{e_{\mathrm{e}}(\alpha+\beta)}\varepsilon_{\mathrm{e}}E_{2,z} + \frac{\varepsilon_{11}^{\mathrm{m}}E_{2,z}}{2}\left(\mathrm{e}^{\mathrm{i}\theta}+\frac{\alpha-\beta}{\alpha+\beta}\mathrm{e}^{-\mathrm{i}\theta}\right)\right]. \quad (37)$$

When $\theta = \pm\pi/2$, as expected, $\mathbf{D}^{\mathrm{m}} = \mathbf{D}^{\mathrm{e}}$. When $\theta = 0$ or $\theta = \pi$, the electric displacement has only a real component as

$$\mathbf{D}^{\mathrm{m}} = \frac{1+\alpha}{\alpha}\left[e_{15}\gamma_{32,z} + E_{2,z}\frac{\alpha\varepsilon_{11}^{\mathrm{m}} - \beta\varepsilon_{\mathrm{e}}e_{15}/e_{\mathrm{e}}}{\alpha+\beta}\right], \quad (38)$$

which is approximately inversely proportional to α. When α approaches zero first, eqn (37) is reduced to

$$\mathbf{D}^{\mathrm{m}} = \varepsilon_{\mathrm{e}}E_{2,z} - \mathrm{i}\left(e_{15}\gamma_{32,z} - \frac{e_{15}\varepsilon_{\mathrm{e}}}{e_{\mathrm{e}}}E_{2,z}\right)\cot\theta. \quad (39)$$

As can be seen in eqn (39), the electric displacement is independent of the permittivity of the hole. The real part of the electric displacement has the same value as that inside the hole, which satisfies the charge-free boundary condition. However, the piezoelectric property induces an electric displacement in the x_1 direction, which has singularities when $\theta = 0$ and π. It should be pointed out that the electric displacement has only singularities in the D_2 component if $\theta = 0$ or $\theta = \pi$ first and then α approaches zero, as shown by eqn (38). If α approaches zero first the electric displacement will have singularities in the D_1 component at crack tips. The inconsistency is caused by the fact that the two apexes of the ellipse become crack tips when α approaches zero. An analytic function has different limits when it approaches a crack tip along different paths. Furthermore, if the permittivity of the hole is treated as zero first, eqn (37) can be simplified to

$$\mathbf{D}^{\mathrm{m}} = \frac{1+\alpha}{\alpha\cos\theta+\mathrm{i}\sin\theta}[e_{15}\gamma_{32,z} + \varepsilon_{11}^{\mathrm{m}}E_{2,z}]\cos\theta. \quad (40)$$

Then, if α approaches zero, eqn (40) is further reduced to

$$\mathbf{D}^{\mathrm{m}} = -\mathrm{i}[e_{15}\gamma_{32,z} + \varepsilon_{11}^{\mathrm{m}}E_{2,z}]\cot\theta. \quad (41)$$

In this case, the electric displacement has no component along the x_2 axis, when the hole surface is approached from the outside. However, eqn (29) shows that the electric displacement inside the hole has only one component in the x_2 direction for any non-zero values of α and β. The electric displacement approaches zero only when the ratio of α/β approaches infinity. An assumption of a zero electric displacement along the crack faces would lead to a zero electric displacement inside the cavity and then a zero electric field strength, which is in contrast to the fact that the electric field strength inside the cavity is uniform and approaches infinity when both α and β approach zero.

5. ENERGY AND ENERGY RELEASE RATE

In order to calculate the energy release rate for crack propagation, energies of the system are first studied. There are two sorts of energies, mechanical and electric, in the system. In both the piezoelectric material and the vacuum elliptic cavity exist electric fields which contribute to the electric energy and then the energy release rate. The two energies of the system per thickness are given by

$$U_{ela} = \int_{\Sigma} \tfrac{1}{2}\boldsymbol{\sigma}_{ij}\mathbf{s}_{ij}\,\mathrm{d}s, \quad U_{ele} = \int_{\Sigma} \tfrac{1}{2}\mathbf{D}_i\mathbf{E}_i\,\mathrm{d}s, \tag{42}$$

where U_{ela} and U_{ele} denote the mechanical and electric energies, respectively, and where the integration covers the total area, Σ, including both the material and the hole. Application of the divergence theorem to U_{ela} and U_{ele} yields

$$U_{ela} = \frac{1}{2}\oint_L \mathbf{n}_i\boldsymbol{\sigma}_{ij}\mathbf{u}_j\,\mathrm{d}l, \quad U_{ele} = -\frac{1}{2}\oint_L \mathbf{n}_i\mathbf{D}_i\phi\,\mathrm{d}l, \tag{43}$$

where the integration contour of a circle, centred at the origin, of radius ρ encloses the entire system. Sih and Liebowitz (1968) calculated the elastic energy in a solid containing an elliptical hole under anti-plane loading. Following their treatments, the two energy functions can be expressed in terms of the complex potentials

$$U_{ela} = \frac{\mathrm{i}}{8}\oint_L [U(z)-\overline{U(z)}]\left[c_{44}U'(z)+e_{15}(\Phi^{m})'(z)-\frac{\rho^2}{z^2}(c_{44}\overline{U'(z)}+e_{15}\overline{(\Phi^{m})'(z)})\right]\mathrm{d}z,$$

$$U_{ele} = \frac{-\mathrm{i}}{8}\oint_L [\Phi^{m}(z)-\overline{\Phi^{m}(z)}]\left[e_{15}U'(z)-\varepsilon_{11}^{m}(\Phi^{m})'(z)-\frac{\rho^2}{z^2}(e_{15}\overline{U'(z)}-\varepsilon_{11}^{m}\overline{(\Phi^{m})'(z)})\right]\mathrm{d}z. \tag{44}$$

Equation (44) shows that the mechanical and electric energies are determined just by the two complex potentials defined in the material domain. In order to calculate the energy change induced by the elliptical hole, the complex potentials have to be readjusted

$$U(z) = \left(A_1-\frac{A_2'}{\rho^2}\right)z+\frac{A_2'}{z}, \quad \Phi^{m}(z) = \left(B_1-\frac{B_2'}{\rho^2}\right)z+\frac{B_2'}{z}, \tag{45}$$

so that the mechanical and electric tractions on the large contour L are in equilibrium with the imposed mechanical and electric loadings at infinity. Comparing eqn (45) with (23), we find relations between these constants with and without a prime:

$$A_2' = R^2A_2-\frac{c^2}{4}A_1, \quad B_2' = R^2B_2-\frac{c^2}{4}B_1. \tag{46}$$

Using eqn (45) and (46) and completing the two integrations of eqn (44) lead to

$$U_{ela} = \frac{\pi}{2}[A_1(c_{44}A_1+e_{15}B_1)\rho^2-2A_2'(c_{44}A_1+e_{15}B_1)], \tag{47}$$

$$U_{ele} = \frac{-\pi}{2}[B_1(e_{15}A_1-\varepsilon_{11}^{m}B_1)\rho^2-2B_2'(e_{15}A_1-\varepsilon_{11}^{m}B_1)], \quad \rho\to\infty.$$

Substituting eqn (46) into eqn (47) results in

$$U_{ela} = \frac{\pi\gamma_{32,\infty}\sigma_{32,\infty}\rho^2}{2} + \frac{\pi a(a+b)\sigma_{32,\infty}}{2}\left[\gamma_{32,\infty} - \frac{(a+b)\beta e_{15}E_{2,\infty}}{(b+a\beta)c_{44}}\right], \tag{48}$$

$$U_{ele} = \frac{\pi E_{2,\infty}D_{2,\infty}\rho^2}{2} + \frac{\pi ab(a+b)E_{2,\infty}D_{2,\infty}}{2}\left[\frac{1-\beta}{b+a\beta}\right].$$

As can be seen in eqn (48), there are two terms in each of the two energies. The first terms represent the energies, mechanical and electric, that the piezoelectric cylinder would possess with no cavity present, and the second terms are the majority of energies due to the presence of the cavity. As an important consequence, the total energy due to the elliptical hole is given by

$$U_t = \frac{\pi a(a+b)}{2}\left[\sigma_{32,\infty}\left(\gamma_{32,\infty} - \frac{(a+b)\beta e_{15}E_{2,\infty}}{(b+a\beta)c_{44}}\right) + bE_{2,\infty}D_{2,\infty}\left(\frac{1-\beta}{b+a\beta}\right)\right]. \tag{49}$$

The energy release rate for crack propagation is defined as the differentiation of the crack induced energy with respect to the crack length. Assuming b remains unchanged during cavity growth, we define the energy release rate, G_h, for the cavity growth as:

$$G_h = \frac{1}{2}\frac{dU_t}{da} = \frac{\pi(2a+b)}{4}\left[\sigma_{32,\infty}\left(\gamma_{32,\infty} - \frac{(a+b)\beta e_{15}E_{2,\infty}}{(b+a\beta)c_{44}}\right) + bE_{2,\infty}D_{2,\infty}\left(\frac{1-\beta}{b+a\beta}\right)\right]$$
$$- \frac{\pi ab(a+b)\beta(1-\beta)E_{2,\infty}}{4}\left[\frac{c_{44}D_{2,\infty} + e_{15}\sigma_{32,\infty}}{(b+a\beta)^2 c_{44}}\right]. \tag{50}$$

If the piezoelectric constant, e_{15}, is zero, eqns (49) and (50) are, respectively, reduced to

$$U_t = \frac{\pi a(a+b)}{2}\left[\sigma_{32,\infty}\gamma_{32,\infty} + bE_{2,\infty}D_{2,\infty}\left(\frac{\varepsilon_{11}^m - \varepsilon_{11}^c}{b\varepsilon_{11}^m + a\varepsilon_{11}^c}\right)\right], \tag{51}$$

$$G_h = \frac{\pi}{4}\left[(2a+b)\sigma_{32,\infty}\gamma_{32,\infty} + bE_{2,\infty}D_{2,\infty}\frac{(\varepsilon_{11}^m - \varepsilon_{11}^c)[b(2a+b)\varepsilon_{11}^m + a^2\varepsilon_{11}^c]}{(b\varepsilon_{11}^m + a\varepsilon_{11}^c)^2}\right]. \tag{52}$$

In this case, the mechanical and electric energies are decoupled, as shown in eqn (51). The two energies correspond respectively to the mechanical and electric loadings, and the electric energy is proportional to the area of the elliptical hole. Equation (52) indicates that the energy release rate for mechanical loading is always positive and is also positive for electric loading, as long as permittivity of the material is larger than that of the cavity.

When b approaches zero, eqns (49) and (50), respectively, will approach

$$U_t = \frac{\pi a^2\sigma_{32,\infty}}{2}\left[\gamma_{32,\infty} - \frac{e_{15}E_{2,\infty}}{c_{44}}\right], \tag{53}$$

$$G_h = \frac{\pi a\sigma_{32,\infty}}{2}\left[\gamma_{32,\infty} - \frac{e_{15}E_{2,\infty}}{c_{44}}\right]. \tag{54}$$

In this sense, both the energy and the energy release rate are independent of the permittivity of the hole. Recall

$$\gamma_{32,\infty} - \frac{e_{15}}{c_{44}} E_{2,\infty} = \frac{\sigma_{32,\infty}}{c_{44}} \tag{55}$$

for all four loading cases. Substituting eqn (55) into eqn (53) and (54) yields

$$U_t = \frac{\pi a^2 \sigma_{32,\infty}^2}{2c_{44}}, \quad G_h = \frac{\pi a \sigma_{32,\infty}^2}{2c_{44}}. \tag{56}$$

Equation (56) shows that both the energy and the energy release rate are positive. The energy release rate is determined only by the applied stress. This phenomenon was found in our previous work (Zhang and Hack, 1992), except for replacing the effective shear modulus by the elastic constant c_{44}. For the four loading cases studied, the energy release rates have the following forms:

$$\begin{aligned}
G_{\text{case 1}} &= \frac{\pi a}{2c_{44}} (\sigma_{32,\infty})^2, \\
G_{\text{case 2}} &= \frac{\pi a}{2c_{44}} (c_{44}\gamma_{32,\infty} - e_{15}E_{2,\infty})^2, \\
G_{\text{case 3}} &= \frac{\pi a}{2c_{44}} (\sigma_{32,\infty})^2, \\
G_{\text{case 4}} &= \frac{\pi a}{2c_{44}} \left(\mu_e \gamma_{32,\infty} - \frac{e_{15}}{\varepsilon_{11}^m} D_{2,\infty}\right)^2.
\end{aligned} \tag{57}$$

It is the effective stress that drives crack propagation (Zhang and Hack, 1992). The electric loadings play a role only under constant strain loading. Under constant stress loading, the energy release rates are independent of the electric field, because the electric energy due to the cavity becomes zero as the cavity reduces to a slit crack. All these aspects were discussed in detail in our previous paper (Zhang and Hack, 1992).

If the permittivity inside the hole is initially treated as zero, eqns (49) and (50) are reduced to

$$\begin{aligned}
U_t &= \frac{\pi a(a+b)}{2} [\sigma_{32,\infty}\gamma_{32,\infty} + E_{2,\infty}D_{2,\infty}], \\
G_h &= \frac{\pi(2a+b)}{4} [\sigma_{32,\infty}\gamma_{32,\infty} + E_{2,\infty}D_{2,\infty}].
\end{aligned} \tag{58}$$

It seems that the mechanical and electric fields decouple in this case, as shown in eqn (58). When b approaches zero, the mechanical and electric energies due to the crack have the values of that stored in a circle of radius a. The energy release rates for the four loading cases are given by

$$\begin{aligned}
G_{\text{case 1}} &= \frac{\pi a}{2\mu_e} \left(\sigma_{32,\infty}^2 + \frac{c_{44}}{\varepsilon_{11}^m} D_{2,\infty}^2\right), \\
G_{\text{case 2}} &= \frac{\pi a}{2} (c_{44}\gamma_{32,\infty}^2 + \varepsilon_{11}^m E_{2,\infty}^2), \\
G_{\text{case 3}} &= \frac{\pi a}{2c_{44}} [(\sigma_{32,\infty} + e_{15}E_{2,\infty})^2 + c_{44}\varepsilon_{11}^m E_{2,\infty}^2], \\
G_{\text{case 4}} &= \frac{\pi a}{2} \left(c_{44}\gamma_{32,\infty}^2 + \frac{(e_{15}\gamma_{32,\infty} - D_{2,\infty})^2}{\varepsilon_{11}^m}\right).
\end{aligned} \tag{59}$$

Equation (59) shows that the electric loadings have a great influence on the energy release rates for both remote stress and strain loadings. For all four loading cases, the energy release rate is always positive.

6. MECHANICAL AND ELECTRIC FIELDS NEAR THE CAVITY IN THE MATERIAL

The mechanical and electric fields are determined by the complex potentials which are given by eqn (13). Both electric field strength and electric displacement inside the cavity are uniform, as described in Section 3. In this section, we analyse the mechanical and electric fields in the material. For simplicity, the superscript m for the electric properties is ignored here. When the origin of the system is moved to the right apex of the ellipse, the electric and mechanical fields are presented in variable, $z' = z - a$, as

$$\gamma = \left[\frac{A_1[z'+a+\sqrt{(z'^2+2az'+b^2)}]}{2} - \frac{2R^2A_2}{z'+a+\sqrt{(z'^2+2az'+b^2)}}\right]\frac{1}{\sqrt{(z'^2+2az'+b^2)}},$$

$$\mathbf{E} = -\left[\frac{B_1[z'+a+\sqrt{(z'^2+2az'+b^2)}]}{2} - \frac{2R^2B_2}{z'+a+\sqrt{(z'^2+2az'+b^2)}}\right]\frac{1}{\sqrt{(z'^2+2az'+b^2)}},$$

$$\boldsymbol{\sigma} = c_{44}\gamma - e_{15}E, \quad \mathbf{D} = e_{15}\gamma + \varepsilon_{11}^{m}E. \tag{60}$$

If z' is real, all four functions are real too, as indicated in eqn (60). In this case, as z' approaches zero along the x_1' axis, the values of the four functions are

$$\gamma = \frac{1+\alpha}{\alpha}\left[\gamma_{32,r} - \frac{e_{15}E_{2,r}}{(\alpha+\beta)c_{44}}\right], \quad \mathbf{E} = \frac{1+\alpha}{\alpha+\beta}E_{2,r}, \tag{61}$$

$$\boldsymbol{\sigma} = c_{44}\gamma - e_{15}E, \quad \mathbf{D} = e_{15}\gamma + \varepsilon_{11}^{m}E.$$

Equation (61) shows that the strain will approach infinity when α approaches zero and β has a finite value. A singular strain causes singularities in stress and electric displacement via Hooke's law and the piezoelectricity, respectively. However, as long as the permittivity of the hole has a non-zero value, the electric field strength is finite no matter how small α is. Let b in eqn (60) approach zero first. Then, the mechanical and electric fields in the material have the following form:

$$\gamma = \left[A_1[z'+a+\sqrt{(z'^2+2az')}] - \frac{a^2A_2}{z'+a+\sqrt{(z'^2+2az')}}\right]\frac{1}{2\sqrt{(z'^2+2az')}},$$

$$\mathbf{E} = -\left[B_1[z'+a+\sqrt{(z'^2+2az')}] - \frac{a^2B_2}{z'+a+\sqrt{(z'^2+2az')}}\right]\frac{1}{2\sqrt{(z'^2+2az')}},$$

$$\boldsymbol{\sigma} = c_{44}\gamma - e_{15}E, \quad \mathbf{D} = e_{15}\gamma + \varepsilon_{11}^{m}E. \tag{62}$$

Consequently, the strain, stress, electric field strength and electric displacement intensity factors may be defined as

$$K_{III}^{\gamma} = \lim_{z'\to 0}\sqrt{(2\pi z')}\gamma_{32}, \quad K_{III}^{\sigma} = \lim_{z'\to 0}\sqrt{(2\pi z')}\sigma_{32},$$

$$K_{III}^{E} = \lim_{z'\to 0}\sqrt{(2\pi z')}E_2, \quad K_{III}^{D} = \lim_{z'\to 0}\sqrt{(2\pi z')}D_2. \tag{63}$$

The relationships between the various intensity factors arise from eqn (62) so that

$$K_{III}^{\sigma} = c_{44}K_{III}, \quad K_{III}^{D} = e_{15}K_{III}. \tag{64}$$

Combining eqn (62) with eqn (63) results in

$$K_{\mathrm{III}}^{\gamma} = \sqrt{(\pi a)}\left[\gamma_{32,\infty} - \frac{e_{15}}{c_{44}} E_{2,\infty}\right] = \frac{\sigma_{32,\infty}\sqrt{(\pi a)}}{c_{44}},$$

$$K_{\mathrm{III}}^{\sigma} = c_{44}\sqrt{(\pi a)}\left[\gamma_{32,\infty} - \frac{e_{15}}{c_{44}} E_{2,\infty}\right] = \sigma_{32,\infty}\sqrt{(\pi a)},$$

$$K_{\mathrm{III}}^{E} = 0,$$

$$K_{\mathrm{III}}^{D} = e_{15}\sqrt{(\pi a)}\left[\gamma_{32,\infty} - \frac{e_{15}}{c_{44}} E_{2,\infty}\right] = \frac{\sigma_{32,\infty}\sqrt{(\pi a)} e_{15}}{c_{44}}. \tag{65}$$

The near crack tip strain, stress and electric displacement may be expressed in terms of the strain, stress and electric displacement factors as

$$\sigma_{32} = \frac{K_{\mathrm{III}}^{\sigma}}{\sqrt{(2\pi r)}}\cos\frac{\theta}{2}, \qquad \sigma_{31} = -\frac{K_{\mathrm{III}}^{\sigma}}{\sqrt{(2\pi r)}}\sin\frac{\theta}{2},$$

$$\gamma_{32} = \frac{K_{\mathrm{III}}^{\gamma}}{\sqrt{(2\pi r)}}\cos\frac{\theta}{2}, \qquad \gamma_{31} = -\frac{K_{\mathrm{III}}^{\gamma}}{\sqrt{(2\pi r)}}\sin\frac{\theta}{2},$$

$$\mathbf{D}_2 = \frac{K_{\mathrm{III}}^{D}}{\sqrt{(2\pi r)}}\cos\frac{\theta}{2}, \qquad \mathbf{D}_1 = -\frac{K_{\mathrm{III}}^{D}}{\sqrt{(2\pi r)}}\sin\frac{\theta}{2}. \tag{66}$$

It should be noted that while eqn (66) expresses the fields around the right crack tip, they obscure the physical parameters which induce those fields. Also, eqn (66) is a good approximation only if the following inequalities

$$\begin{aligned} &r \ll a \quad \text{for} \quad \gamma, \\ &r \ll a \quad \text{and} \quad \gamma \gg \frac{e_{15}E}{c_{44}} \quad \text{for} \quad \boldsymbol{\sigma}, \\ &r \ll a \quad \text{and} \quad \gamma \gg \frac{\varepsilon_{11}^{\mathrm{m}}E}{e_{15}} \quad \text{for} \quad \mathbf{D}, \end{aligned} \tag{67}$$

are valid. Consequently, the energy release rate, eqn (56), can be represented in terms of the stress intensity factor

$$G_{\mathrm{III}} = \frac{(K_{\mathrm{III}}^{\sigma})^2}{2c_{44}}. \tag{68}$$

When the permittivity of the hole is treated as zero first, then $A_2 = -A_1$ and $B_2 = -B_1$. In this case, b approaching zero reduces eqn (60) to

$$\gamma = \frac{A_1}{2}\left[[z' + a + \sqrt{(z'^2 + 2az')}] + \frac{a^2}{z' + a + \sqrt{(z'^2 + 2az')}}\right]\frac{1}{\sqrt{(z'^2 + 2az')}},$$

$$\mathbf{E} = -\frac{B_1}{2}\left[[z' + a + \sqrt{(z'^2 + 2az')}] + \frac{a^2}{z' + a + \sqrt{(z'^2 + 2az')}}\right]\frac{1}{\sqrt{(z'^2 + 2az')}},$$

$$\boldsymbol{\sigma} = c_{44}\gamma - e_{15}E, \quad \mathbf{D} = e_{15}\gamma + \varepsilon_{11}^{\mathrm{m}}E. \tag{69}$$

Then, the various intensity factors are derived from eqns (69) and (63). They are given by

$$K^{\gamma}_{\mathrm{III}} = \sqrt{(\pi a)}\gamma_{32,x}, \quad K^{\sigma}_{\mathrm{III}} = \sqrt{(\pi a)}\sigma_{32,x},$$
$$K^{E}_{\mathrm{III}} = \sqrt{(\pi a)}E_{2,x}, \quad K^{D}_{\mathrm{III}} = \sqrt{(\pi a)}D_{2,x}. \tag{70}$$

Equation (70) shows that the electric field strength factor is no longer zero. The relationships between the intensity factors are exactly the same as these between the properties. Furthermore, the energy release rate, eqn (58), is re-expressed in terms of the intensity factors as

$$G_{\mathrm{III}} = \frac{K^{\sigma}_{\mathrm{III}}K^{\gamma}_{\mathrm{III}} + K^{D}_{\mathrm{III}}K^{E}_{\mathrm{III}}}{2}. \tag{71}$$

It should be pointed out that eqn (71) differs from that in some previous works (Pak, 1990; Suo *et al.*, 1992). In the present work, the energy release rate is a sum of the mechanical intensity factor product plus the electric intensity factor product; but in the previous works, G equals the mechanical intensity factor product minus the electric intensity factor product (Pak, 1990; Suo *et al.*, 1992). The reason for the inconsistency is that in the previous works (Pak, 1990; Suo *et al.*, 1992), an electric enthalpy, which is not positively definite, was used to calculated the energy release rate.

7. DISCUSSION

The material properties of piezoelectric ceramics (e.g. lead zirconate titanate) are given below (Pak, 1990):

$$c_{44} = 3.53\times 10^{10}\frac{N}{m^2},$$
$$e_{15} = 17.0\frac{C}{m^2},$$
$$\varepsilon^{\mathrm{m}}_{11} = 151\times 10^{-10}\frac{C}{Vm},$$
$$\varepsilon^{\mathrm{e}}_{11} = 8.85\times 10^{-12}\frac{C}{Vm}, \tag{72}$$

where N is the force in newtons, C is the charge in coulombs, V is the electric potential in volts and m is the length in metres. The permittivity of free space is also given in eqn (72). From these data, the effective dielectric constant, the effective shear modulus, the effective piezoelectric constant and the dimensionless constant β are evaluated.

$$\varepsilon_{\mathrm{e}} = 233\times 10^{-10}\frac{C}{Vm}, \quad \mu_{\mathrm{e}} = 5.44\times 10^{10}\frac{N}{m^2}, \quad e_{\mathrm{e}} = 48.4\frac{C}{m^2}, \quad \beta = 3.8\times 10^{-4}. \tag{73}$$

Consider the electric displacement inside the cavity again, when the cavity is reduced to a crack. Assume that the width of a slit crack is on the order of nanometre, i.e. $b = 10^{-9}$ m. If the crack length is on the order of micrometre, i.e. $a = 10^{-6}$ m, then the dimensionless parameter $\alpha = 10^{-3}$ is much smaller than one. The ratio of α over β equals 2.63, which is comparable with one. In this sense, the electric displacement is given by the second limit in eqn (30). To ensure approximately the third limit in eqn (30), $\alpha \to 0$ and $\alpha/\beta \to \infty$, α/β must be larger than 100 and α must be smaller than 0.01. $\alpha/\beta = 100$ yields $\alpha = 0.04$ which is obviously larger than 0.01. This result indicates that the condition for the third limit in eqn (30) cannot be satisfied. When α is smaller than 10^{-6}, then $\alpha/\beta = 2.6\times 10^{-3}$ can be treated as zero. This requires $a = 1$ mm for a nanometre-wide crack.

The energy release rate, i.e. eqn (50), can be re-expressed as

$$G_{\mathrm{h}}=\frac{\pi a}{4}\left[(2+\alpha)\left[\sigma_{32,\infty}\left(\gamma_{32,\infty}-\frac{(1+\alpha)e_{15}E_{2,\infty}}{(1+\alpha\beta)c_{44}}\right)+E_{2,\infty}D_{2,\infty}\left(\frac{1-\beta}{1+\beta/\alpha}\right)\right]\right.$$
$$\left.-(1+\alpha)(1-\beta)E_{2,\infty}\frac{c_{44}D_{2,\infty}+e_{15}\sigma_{32,\infty}}{(1+\alpha/\beta)^2c_{44}}\alpha/\beta\right]. \quad (74)$$

When both α and β are much smaller than one, eqn (74) is reduced to

$$G_{\mathrm{h}}=\frac{\pi a}{2}\left[\sigma_{32,\infty}\left(\gamma_{32,\infty}-\frac{e_{15}E_{2,\infty}}{(1+\alpha/\beta)c_{44}}\right)+\frac{E_{2,\infty}D_{2,\infty}}{1+\beta/\alpha}-E_{2,\infty}\frac{c_{44}D_{2,\infty}+e_{15}\sigma_{32,\infty}}{2(1+\alpha/\beta)^2c_{44}}\alpha/\beta\right]. \quad (75)$$

Only when α/β is much smaller than one can eqn (75) be reduced further to eqn (54). Since the condition that α/β is much larger than one may not be satisfied for a slit crack, as discussed above, the energy release rate given in eqn (59) may not hold for real materials.

8. SUMMARY

The mechanical and electric fields in a piezoelectric material containing an elliptical cylinder hole under anti-plane mechanical loading and in-plane electric loading were formulated by complex variables. The total energy induced by the elliptical cavity was evaluated and the energy release rate was analysed. The solution to a mode III piezoelectric fracture problem was obtained by letting the short semi-axis of the ellipse approach zero. The results show that if the ratio of the short semi-axis over the length semi-axis, α, is much smaller than the ratio of the permittivity of the cavity over the effective dielectric constant of the material, β, then:

(1) the electric boundary condition along the crack faces may be given as the electric field strength equals the remote applied one, as shown in eqn (33);

(2) strain, stress and electric displacement intensity factors can be introduced to measure the strengths of the corresponding singularities at the crack tips, but the electric field strength does not produce any singularity; and

(3) the energy release rate is always positive and has the same form as given in our previous work (Zhang and Hack, 1992) except for replacing the effective shear modulus by the elastic constant, c_{44}.

Acknowledgement Financial support from the Hong Kong Research Grants Council via a Competitive Earmarked Research Grant, HKUST573/94E, is gratefully acknowledged.

REFERENCES

Barnett, D. M. and Lothe, J. (1975). Dislocations and line charges in anisotropic piezoelectric insulators. *Phys. Status Solidi (b)* **67**, 105–111.

Deeg, W. F. (1980). The analysis of dislocation, crack and inclusion problems in piezoelectric solids. Ph.D Thesis, Stanford University.

Dunn, M. (1994). The effects of crack face boundary conditions on the fracture mechanics of piezoelectric solids. *Engng Fracture Mech.* **48**, 25–39.

Jackson, J. D. (1976). *Classical Electrodynamics*. John Wiley, New York.

Kuo, C.-M. and Barnett, D. M. (1991). *Modern Theory of Anisotropic Elasticity and Applications* (Edited by J. J. Wu, T. C. T. Ting and D. M. Barnett), SIAM Proceedings, pp. 35–50.

McMeeking, R. M. (1989). Electrostrictive stresses near crack-like flaws. *J. Appl. Math. Phys.* **40**, 615–627.

Pak, Y. E. (1990). Crack extension force in a piezoelectric material. *J. Appl. Mech.* **57**, 647–653.

Pak, Y. E. (1992). Linear electroelastic fracture mechanics of piezoelectric materials. *Int. J. Fracture* **54**, 79–100.

Pak, Y. E. and Tobin, A. (1993). On electric field effects in fracture of piezoelectric materials. *Mech. Electromagn. Mater. Structures* **AMD 161/MD 42**, 51–62.

Park, S. (1994). Fracture behaviour of piezoelectric materials. Ph.D. Thesis, Purdue University.

Parton, V. Z. (1976). Fracture mechanics of piezoelectric materials. *Acta Astronaut.* **3**, 671–683.

Parton, V. Z. and Kudryavtsev, B. A. (1988). *Electromagnetoelasticity Piezoelectrics and Electrically Conductive Solids*. Gordon and Breach, New York.

Shindo, Y., Ozawa, E. and Nowacki, J. P. (1990). Singular stress and electric fields of a cracked piezoelectric strip. *Appl. Electromagn. Mater.* **1,** 77–87.

Sih, G. C. and Liebowitz, H. (1968). Mathematical theories of brittle fracture. In *Fracture. An Advanced Treatise* (Edited by H. Liebowitz), Vol. II, 67–190. Academic Press, New York.

Sosa, H. A. (1993). Crack problems in piezoelectric ceramics. *Mech. Electromagn. Mater. Structures* **AMD 161/MD 42,** 63–75.

Sosa, H. A. and Pak, Y. E. (1990). Three-dimensional eigenfunction analysis of a crack in a piezoelectric material. *Int. J. Solids Structures* **26,** 1–15.

Suo, Z., Kuo, C.-M., Barnett, D. M. and Willis, J. R. (1992). Fracture mechanics for piezoelectric ceramics. *J. Mech. Phys. Solids* **40,** 739–765.

Zhang, T.-Y. (1994a). Effects of sample width on the energy release rate and electric boundary conditions along crack surfaces in piezoelectric materials. *Int. J. Fracture* **66,** R33–R38.

Zhang, T.-Y. (1994b). *J*-integral measurement for piezoelectric materials. *Int. J. Fracture* **68,** R33–R40.

Zhang, T.-Y. and Hack, J. E. (1992). Mode-III cracks in piezoelectric materials. *J. Appl. Phys.* **71,** 5865–5870.

Zhang, T.-Y. and Tong, P. (1995). Linear fracture mechanics for piezoelectric materials, unpublished work.